LETTER TO THE EDITOR

What can we learn from double-electron emission by one circularly polarized photon?

Jamal Berakdar†
Max-Planck-Institut für Mikrostrukturphysik, Weinberg 2, 06120 Halle, Germany

Received 8 October 1998, in final form 27 November 1998

Abstract. Using a simple exact analysis of the one-photon optical transition amplitudes for the emission of correlated electron pairs from randomly oriented targets it is shown that information on the phase differences of these amplitudes can be obtained by the variation of the helicity of the absorbed photon. Experiments performed with different polarization of the photon can be related to each other by analytical formulae that should be used as a consistency check. The usefulness of this approach is demonstrated by analysing recent experimental and theoretical data.

Single-photoelectron spectroscopy in the ultraviolet regime has emerged as a powerful technique for the investigation of electronic and structural properties of materials [1]. An important feature of the photoelectron-emission process is the dependence of the photoelectron spectra on the polarization state of the photon, photoelectron and/or residual ion. For a circularly polarized photon, the dependence on the photon's helicity has been dubbed *circular dichroism* (CD) and has been the subject of a number of studies on the direct photoelectron emission as well as on the resonant ionization with photoexcitation of an autoionizing state (see [2–4] and references therein).

For single-photoelectron emission from a randomly oriented target and under the assumption that the ion's final-state magnetic sublevels are not resolved, the angular distribution of the *spin non-resolved* photoelectrons is given by [5] (a first-order perturbative treatment and the dipole approximation are used for the radiation field, atomic units (au) are used throughout)

$$\frac{\mathrm{d}\sigma}{\mathrm{d}\Omega_{\mathrm{p}}} = \frac{\sigma_0}{4\pi}\left[1 - \tfrac{1}{2}\beta P_2(\hat{\boldsymbol{k}}\cdot\hat{\boldsymbol{p}})\right]. \qquad (1)$$

Here σ_0 is the total cross section, Ω_{p} is the solid ejection angle of the photoelectron emitted with momentum $\boldsymbol{p}$, β is the asymmetry parameter, $\hat{\boldsymbol{k}}$ is the direction of incident light and P_2 is the second Legendre polynomial. Equation (1) holds for right and left circularly polarized light as well as for unpolarized light, i.e. the helicity of the light has no dynamical effect and the CD is absent in this case. In fact, for linearly polarized light, the photoelectron angular distributions are obtained from equation (1) upon replacing β by -2β and $\hat{\boldsymbol{k}}$ by the direction of the electric field strength. Additional information can be obtained by analysing the spin states of the photoelectron [6], yet the polarization of the photon does not yield any further insight.

This situation changes radically when *two* photoelectrons are emitted simultaneously upon single-photon absorption. The angular and energy distributions of the photoelectrons reveal

† E-mail address: jber@mpi-halle.de

0953-4075/99/020027+07$19.50

a strong dependence on the helicity of the photon [7–13]. In this case, employing a formal analysis, the symmetry properties of the CD have been established [7, 8] and the signature of electronic correlation has been exposed [14]. A non-vanishing CD in the two-electron emission requires that the photoelectrons' vector momenta, $\boldsymbol{k}_a$ and $\boldsymbol{k}_b$, and the wavevector of the photon, $\boldsymbol{k}$, are linearly independent. In addition, the two electrons have to escape with unequal energies. It should be noted, however, that these conditions are necessary but not sufficient for a non-vanishing CD, i.e. the CD might still diminish for dynamical reasons at certain points whose positions are very much dependent on the calculational scheme used [14].

In this work we are concerned with the questions: (a) which measurable physical quantities can be extracted from the CD? and (b) how can we relate experiments with linearly polarized photons with those performed using circularly polarized light? To shed light on these questions we write the photo-double-emission (PDE) cross section, that is differential in the solid angles Ω_a, Ω_b and energies E_a, E_b of the emitted electrons, in the form

$$\sigma(\Omega_a, \Omega_b, E_b) = C \sum_{M_f} \frac{1}{2J_i + 1} \sum_{M_i} |T|^2 \tag{2}$$

where T is the optical transition amplitude, $C = 4\pi^2 \alpha_c k_a k_b \omega$, $k_{a/b} = \sqrt{2E_{a/b}}$, α_c is the fine-structure constant and ω is the frequency of the light. Equation (2) averages over the initial magnetic sublevels M_i, and sums over the magnetic sublevels M_f of the target final states. In this paper, numerical examples will be presented for a He target in its ground state so that the summation in equation (2) over M_f disappears. As is well known, the circular polarized state of the photons can be constructed from two independent linearly polarized states. Using a coordinate system where the z-axis is aligned along the wavevector of the circular photon, the optical transition amplitude with left- (right-) hand circularly polarized light, labelled as T_{σ^+} (T_{σ^-}), can thus be written as

$$T_{\sigma^\pm} = c(T_x \pm \mathrm{i} T_y). \tag{3}$$

Here, T_x (T_y) is the transition amplitude for the DPE with linearly polarized light where the electric field vector is aligned along the x (y) direction and $c = 1/\sqrt{2}$. The photoelectrons are emitted with momenta $\boldsymbol{k}_a$ and $\boldsymbol{k}_b$ determined in the coordinate system x, y, z. For the following it is instructive to write equation (3) in the form

$$T_{\sigma^\pm} = c[|T_x| \exp(\mathrm{i}\phi_x) + |T_y| \exp(\mathrm{i}\phi_y \pm \mathrm{i}\pi/2)] \tag{4}$$

where ϕ_x (ϕ_y) is the phase of T_x (T_y). Thus, the quantities $|T_{\sigma^\pm}|^2$ that determine the cross section (2) attain the form

$$|T_{\sigma^\pm}|^2 = \tfrac{1}{2}\big[|T_x|^2 + |T_y|^2 \pm 2|T_x||T_y| \sin(\phi_y - \phi_x)\big]. \tag{5}$$

Now, if we define the CD as CD $:= (\sigma^+ - \sigma^-)/(\sigma^+ + \sigma^-)$ where σ^+ (σ^-) is the PDE cross section upon the absorption of a photon with positive (negative) helicity then we obtain from equation (5)

$$\mathrm{CD} = \frac{2|T_x||T_y|}{|T_x|^2 + |T_y|^2} \sin(\phi_y - \phi_x). \tag{6}$$

Equivalently, one can show that

$$\mathrm{CD} = -\frac{2}{|T_x|^2 + |T_y|^2} \, \mathrm{Im}(T_y T_x^*). \tag{7}$$

To quantify the non-interference terms in equation (5) one should inspect the quantity

$$\Sigma := |T_{\sigma^+}|^2 + |T_{\sigma^-}|^2 = |T_x|^2 + |T_y|^2. \tag{8}$$

This expression for Σ is helicity independent, which is in line with the symmetry properties of $T_{\sigma^\pm}$ [7, 8]. From an experimental point of view, equation (8) is useful in so far as it can be used to check the consistency of the data when measuring $|T_{\sigma^\pm}|^2$ and $|T_{x/y}|^2$, as is done below.

From equation (6) it is obvious that:

(a) The CD vanishes for $\phi_y - \phi_x = n\pi$ and n is an integer, this is for example the case where T_y and T_x are both pure imaginary or pure real.
(b) The CD vanishes when T_x and/or T_y vanishes.
(c) The CD diminishes as $|T_l|/|T_j|$; $j = x, y$; $l = y, x$ for $|T_j| \gg |T_l|$.

From the above equations we conclude further that by changing the polarization states of the photons information on the *phase differences* of the optical transition amplitudes can be obtained. As mentioned above this is in contrast to single-photoelectron emission where *such* a phase difference of the transition amplitude is inaccessible experimentally (note we are dealing here with isotropic targets with the spin states of the photoelectron and the final ion magnetic sublevels not being resolved, in contrast phase shift differences between partial waves can be determined from the angular distribution and a spin polarization analysis of the photoelectron).

To demonstrate the usefulness of the above simple analysis let us consider a prototype case where $|T_{x,y,\sigma^\pm}|$, Σ and the CD have been measured. All calculations have been performed using the technique outlined in [7, 8]. The final state has been modelled by a product of two plane waves modified by three two-body Coulomb distorting factors, the so-called 3C approximation [15–17].

As seen in figures 1(*a*) and (*b*), the *shape* of the experimental findings for $|T_x|^2$ and $|T_y|^2$ is reasonably reproduced by the theory, however, considerable deviations between theory and experiment are observed as far as the magnitude of the cross sections is concerned. This is most likely to be due to a shortcoming of the present calculational scheme. At $\varphi_a = 0, \pi, 2\pi$ the amplitude T_y possesses a zero point, since in this case the two photoelectrons escape perpendicular to the linear polarization vector [17]. Generally, a *shape* agreement between theory and experiment, as far as $|T_x|^2$ and $|T_y|^2$ are concerned, does not mean the same kind of agreement for the sum Σ of $|T_x|^2$ and $|T_y|^2$ (figure 1(*c*)), for the shape of Σ depends on the relative ratio between $|T_x|^2$ and $|T_y|^2$. As remarked above, according to equation (8) Σ should be helicity independent. This means that the experimental Σ as deduced from the measurements shown in figure 1(*a*) and those in figure 1(*e*) ($\sigma^\pm$) should be the same. Unfortunately, as seen in figure 1(*c*), such a comparison of the measurements seems to be inconsistent with equation (8). The reason for this has yet to be clarified.

Comparing figures 1(*a*) and (*b*) [$|T_{x/y}|^2$] and figure 1(*c*) (Σ) it is evident that the minimum in Σ at $\varphi_a = \pi$ is due to the zero point in T_y at the same position, whereas the two peaks originate from the corresponding peaks in $|T_y|^2$ (more precisely the peaks in Σ at $\varphi_a \approx 125^\circ, 235^\circ$ are due to the dip in Σ at $\varphi_a = \pi$!).

As is evident from equation (5), the difference between Σ, as depicted in figure 1(*c*), and $\sigma^\pm$ is controlled by the interference term between T_x and T_y, and therefore by the phase difference $\phi_{yx} := \phi_y - \phi_x$. As seen in figure 1(*d*), ϕ_{yx} remains almost unchanged when using different initial-state descriptions, in contrast to Σ (cf figure 1(*c*)). From figure 1(*d*) we also notice that when both electrons emerge approximately in the same direction (i.e. in the region $260^\circ < \varphi_a < 100^\circ$), the phase difference ϕ_{yx} is relatively small and smooth. As a result, the cross sections $\sigma^\pm$ (see figure 1(*e*)) are basically dictated by Σ (which is helicity independent) and consequently do not differ much from each other. On the other hand, when the photoelectrons escape almost opposite to each other ($\varphi_a \approx 180^\circ$), we observe a considerable phase difference ϕ_{yx} (cf figure 1(*d*)). As is obvious from the sign of ϕ_{yx} this results, as far as σ^+ is concerned, in a constructive (destructive) interference of T_x and T_y for $\varphi_a < 180^\circ$

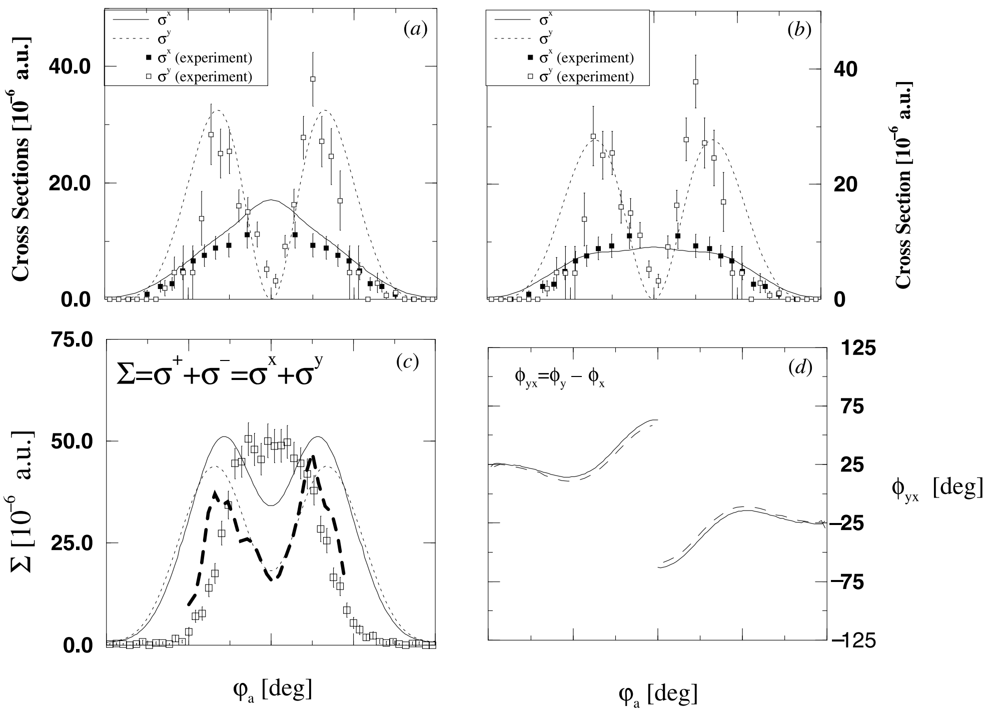

Figure 1. (*a*) The cross sections for double ionization of He($^1S^e$) with a linear polarized photon are shown. Two cases are depicted in which the photon's polarization vector is fixed along the x (full curve, labelled σ^x) or the y-direction (dotted curve, labelled σ^y). The excess energy is 20 eV. Both ejected electrons are detected in the x–y plane. One fast electron (electron b with 17.5 eV) is detected along the x-direction, whereas the angular distribution of the slower one (electron a) is scanned with φ_a being its (positive) azimuth angle (with respect to the x-axis). Experimental data are provided by Bräuning *et al* [18]. In the calculations, the finite energy resolution of ± 1 eV has not been taken into account. The initial state has been modelled by a three-parameters Hylleraas wavefunction [14, 19], whereas the final state is taken as a 3C wavefunction (see text). The velocity form has been employed. (*b*) Same geometry and notation as (*a*), but the initial state has been modelled by a wavefunction that partially satisfies the two-body cusp conditions as proposed in [20]. To allow for shape comparison the full curves in (*a*) and (*b*) have been multiplied by a factor of 2 and the dotted curve by a factor of 4. The experimental data are on an absolute scale. (*c*) The sum Σ ($\Sigma = \sigma^x + \sigma^y = \sigma^- + \sigma^+$) for the detection geometry as in (*a*). The full curve has been obtained using the same theoretical model as in (*a*), whereas the dotted curve derives from the theory of (*b*). The theoretical results have been multiplied by a factor of 4. The thick broken curve is the (absolute) experimental Σ as deduced from (*a*), whereas the open squares are the (absolute) experimental value for Σ as deduced from the measured $\sigma^{\pm}$ (cf (*e*)). According to (8) the experimental curves should be equivalent. (*d*) The differences $\phi_{yx} = \phi_y - \phi_x$ of the phases ϕ_y and ϕ_x of the amplitudes T_y and T_x, as used to calculate σ^y and σ^x, respectively. The full (broken) curve corresponds to the case of (*a*) (part (*b*)). (*e*) The same arrangement of the electron detectors, however, the photon is circularly polarized with its wavevector pointing along the z-direction. Cross sections for positive (full curve, labelled σ^+) and negative (dotted curve, labelled σ^-) helicity photons are depicted. The calculations are as in (*a*) except for the broken curve where σ^+ has been evaluated using for the initial-state description the wavefunction proposed in [20] (same as in (*b*)). Absolute experimental data (full squares for σ^+ and open squares for σ^-) are provided by Mergel *et al* [12]. (*f*) CD as defined by equation (6) for the case of (*e*). The full curve is the CD deduced from the full and the dotted curves in (*e*), whereas the broken curve corresponds to the CD as predicted by the calculation labelled by the broken curve in (*e*). The experimental values correspond to those depicted in (*e*).

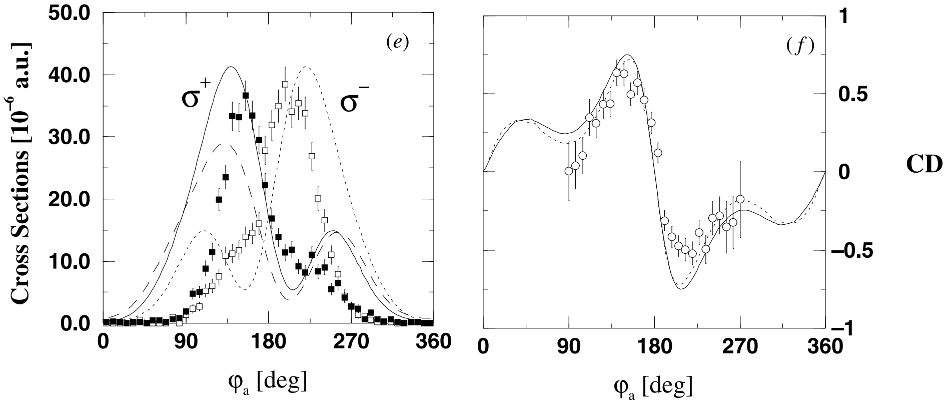

Figure 1. Continued.

($\varphi_a > 180°$) leading the shape of σ^+, as observed in figure 1(*e*). The same consideration applies to σ^-. Therefore, one can conclude that the structure of the angular distribution of $\sigma^\pm$ (two peaks and one minimum) has its origin in the shape of Σ, superimposed on that of the interference pattern of T_x and T_y. The origin of the structures in Σ has been explored above. The discrepancies between theory and experiment, as far as the shape is concerned, remain to be clarified, in particular, in view of the observations made in figure 1(*c*) and the approximate theoretical model.

The explanation of the shape of ϕ_{yx}, as shown in figure 1(*d*), is a delicate problem since ϕ_{yx} is a dynamical quantity and is independent of $|T_{x/y}|$. What I can remark here is only that the symmetry properties of ϕ_{yx} are directly linked to those of the CD via equation (6), i.e. the reflection symmetry of ϕ_{yx} with respect to $\varphi_a = 0°$ and 180° (and hence the discontinuity at these points) is readily explained by the symmetry property of the CD, namely, $\mathrm{CD}(\phi_y - \phi_x) = -\mathrm{CD}(\phi_x - \phi_y)$ (since $T_y = 0$ at $\varphi = 0, \pi$ these points have to be excluded from equation (6)).

As deduced from equation (6), the structure of the CD is the result of an interplay of two effects: the ratio between the geometrical and the arithmetical average of $|T_x|^2$ and $|T_y|^2$, on the one hand, and the value of ϕ_{yx}, on the other hand. The former is largest when $|T_x|$ and $|T_y|$ are equal. Therefore, we observe two maxima in the CD approximately at the positions where $|T_x|$ crosses $|T_y|$ in figures 1(*a*) and (*b*). The relative heights of these two maxima and the sign of the CD is decided by ϕ_{yx}, as readily seen from figures 1(*d*) and (*f*).

The cross sections $\sigma^\pm$ depend on the *absolute* values of $|T_{x/y}|$ and ϕ_{yx}, whereas the CD does not contain as much precise information on $|T_{x/y}|$. Therefore, $\sigma^\pm$ are more sensitive to the details of the dynamical description than the CD. This is demonstrated in figures 1(*e*) and (*f*) where modelling the initial state by a different wavefunction leads to larger deviations in σ^+ than in the CD.

In the above analysis we used $|T_{x/y}|$ and ϕ_{yx} (figures 1(*a*), (*b*) and (*d*)) to explain the behaviour of $\sigma^\pm$ and the CD. Conversely, and as is evident from equation (5), one can use the measured $|T_{x/y}|$ and, optionally, σ^+ to extract the phase difference ϕ_{yx}. In addition, one might consider $|T_{x/y}|^2$ and the CD as reliable quantities and construct $\sigma^\pm$ according to equation (5).

It is worthwhile to note that equation (8) can be used to check the internal consistency of $|T_x|$ and $|T_y|$. To see this let us consider the situation where both electrons are detected in the x–y plane. In this case one can show that $T_{\sigma^\pm}(\varphi_a - \varphi_b) = T_{\sigma^\pm}(\varphi_a' - \varphi_b')$, for

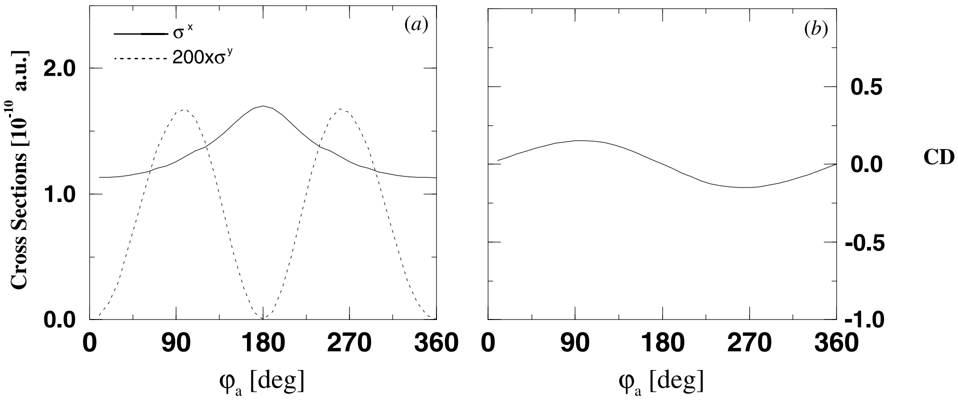

Figure 2. (*a*) The same scattering geometry as in figure 1(*a*) with the same notation and the same theoretical model. The excess energy is, however, 3080 eV. The fast electron (≈3000 eV) is detected along the x-direction, whereas the angular distribution of the slower one (1 eV) is scanned as a function of φ_a. The amplitude $|T_y|$ has been multiplied by a factor of 200 to allow for shape comparison. (*b*) The circular dichroism CD for the detection geometry as in (*a*) but with the photon circularly polarized and its wavevector aligned along the z-direction (cf figure 1(*e*)).

all azimuthal angles $\varphi_a', \varphi_b', \varphi_a, \varphi_b \in [0, 2\pi]$ that satisfy $\varphi_a - \varphi_b = \varphi_a' - \varphi_b'$, i.e. $T_{\sigma^\pm}$ depend on the inter-electronic relative angle only. Therefore, according to equation (8), $\Sigma(\varphi_a - \varphi_b) = \Sigma(\varphi_a' - \varphi_b') = |T_x(\varphi_a - \varphi_b)|^2 + |T_y(\varphi_a - \varphi_b)|^2 = |T_x(\varphi_a' - \varphi_b')|^2 + |T_y(\varphi_a' - \varphi_b')|^2$. The latter relation is important in so far as $T_{x/y}(\varphi_a - \varphi_b) \neq T_{x/y}(\varphi_a' - \varphi_b')$ for $\varphi_{a/b} \neq \varphi_{a/b}'$ and can thus be used to check the consistency of the measured $|T_x|$ and $|T_y|$.

An example of interest that can be explained by exploiting the above equations is that when one very fast electron, say electron b (fast with respect to the second ejected one) escapes along the x (or y) direction. One can argue here that the fast electron absorbs the photon and the second one is ejected with the characteristics of the initial state, which is spatially isotropic. Under these circumstances (one electron is an s electron) the formally exact analysis [7, 8] predicts a vanishing CD. The above (exact) analysis also anticipates a diminishing CD, however, for another reason: regardless of the ejection angle of the slow electron (electron a) the amplitude $|T_x|$ is more than two orders of magnitude larger than $|T_y|$ (cf figure 2(*a*)). This is understandable since the fast electron is fixed along the x-direction. As outlined above, equation (6) then requires that the CD has to decline as $|T_y|/|T_x|$, and therefore the behaviour seen in figure 2(*b*). We note that the angular distribution of $|T_x|$ (as a function of φ_a) is quite smooth (see figure 2(*a*)). In contrast, $|T_y|^2$ as a function of φ_a is not isotropic, in fact, $|T_y|^2$ must have zero points at $\varphi_a = 0, \pi, 2\pi$ (this means that a strict isotropic angular distribution of the slow electron implies $T_y \equiv 0$). Since $|T_x|^2 \gg |T_y|^2$, however, $\sigma^\pm$ and Σ are smooth functions of φ_a (in the extreme case of $|T_y|/|T_x| \to 0$ we arrive at $T_{\sigma^\pm} = T_x/\sqrt{2}$ and the DPE process is directly related to a single-photoelectron emission process that shows no CD).

In summary, using a simple analysis, we have shown that for PDE from isotropic targets (and the random final ion), information on the phase difference of the optical transition amplitudes can be obtained by varying the helicity of the ionizing radiation. No spin-polarization analysis of the photoelectrons is needed. The structure of the cross section for PDE with polarized light can be explained by two (complex) transition amplitudes for PDE via the absorption of linearly polarized light where the linear polarization vectors are perpendicular to each other. A generalization of the present study to the elliptical polarization state of the photon is straightforward.

I would like to thank H Bräuning, M Achler, V Mergel, and R Dörner for communicating their data.

References

[1] Braun J 1996 *Rep. Prog. Phys.* **59** 1267
[2] Baier S, Grum-Grzhimailo A N and Kabachnik N M 1994 *J. Phys. B: At. Mol. Opt. Phys.* **27** 3363–88
[3] Cherepkov N A 1983 *Adv. At. Mol. Phys.* **19** 395–447
Cherepkov N A, Kuznetsov V V and Verbitskii V A 1995 *J. Phys. B: At. Mol. Opt. Phys.* **26** 1221–39
[4] Venus D, Kuch W, Lin T-M, Schneider C M, Ebert H and Kirschner J 1997 *Phys. Rev.* B **55** 2594
[5] Jacobs V L 1972 *J. Phys. B: At. Mol. Phys.* **5** 2257
[6] Klar H 1980 *J. Phys. B: At. Mol. Phys.* **13** 3117 and references therein
[7] Berakdar J and Klar H 1992 *Phys. Rev. Lett.* **69** 1175
[8] Berakdar J, Klar H, Huetz A and Selles P 1993 *J. Phys. B: At. Mol. Opt. Phys.* **26** 1463
[9] Kabachnik N M and Schmidt V 1995 *J. Phys. B: At. Mol. Opt. Phys.* **28** 233
[10] Manakov N L, Marmo S I and Meremianin A V 1996 *J. Phys. B: At. Mol. Opt. Phys.* **29** 2711
[11] Viefhaus J *et al* 1996 *Phys. Rev. Lett.* **77** 3975
[12] Mergel V *et al* 1998 *Phys. Rev. Lett.* **80** 5301
[13] Kheifets A S and Bray I 1998 *Phys. Rev. Lett.* at press
[14] Berakdar J 1998 *J. Phys. B: At. Mol. Opt. Phys.* **31** 3167
[15] Garibotti G and Miraglia J E 1980 *Phys. Rev.* A **21** 572
[16] Brauner M, Briggs J S and Klar H 1989 *J. Phys. B: At. Mol. Opt. Phys.* **22** 2265
[17] Maulbetsch F and Briggs J S 1995 *J. Phys. B: At. Mol. Opt. Phys.* **28** 551
[18] Bräuning H Private communication
Bräuning H *et al* 1998 *J. Phys. B: At. Mol. Opt. Phys.* **31** at press
[19] Hylleraas E A 1929 *Z. Phys.* **54** 347
[20] Bhattacharyya S, Bhattacharyya A, Talukdar B and Deb N C 1996 *J. Phys. B: At. Mol. Opt. Phys.* **29** L147